

Mathematical Analysis of Blood Flow through Stenosed Arteries with Body Acceleration

D.S. Sankar

School of Mathematical Sciences, University Science Malaysia, 11800 Penang, Malaysia
E-mail: sankar_ds@yahoo.co.in

ABSTRACT

The mathematical analysis discusses the pulsatile flow of blood through stenosed narrow artery with body acceleration, treating blood as Herschel-Bulkley fluid. Perturbation method is used to solve the resulting system of nonlinear partial differential equations with appropriate boundary conditions and analyze the flow. The expressions for the shear stress, velocity, flow rate, wall shear stress, plug core radius and longitudinal impedance have been obtained. The variations of these flow quantities with various parameters involved in the fluid flow have been analyzed. It is found that the velocity and flow rate increase with the increase of the pressure gradient, body acceleration and pulsatile Reynolds number and they decrease with the increase of the yield stress and depth of the stenosis. It is noted that the plug core radius and wall shear stress increase with the increase of the yield stress and depth of the stenosis and they decrease with the increase of the body acceleration and pulsatile Reynolds number.

Keywords: Pulsatile Blood Flow, H-B Fluid, Stenosed Artery, Perturbation Method, Longitudinal Impedance.

1. INTRODUCTION

Our body is subject to the body accelerations or vibrations in many situations, like swinging of kids in a cradle, vibration therapy applied to a patient with heart disease etc. [1]. Prolonged exposure to high level unintended external body accelerations may cause serious diseases due to the disturbance in blood flow [2]. Some of the symptoms which result from prolonged body acceleration are headache, abdominal pain, increase in pulse rate, venous pooling of blood in the extremities, loss of vision, hemorrhage in the face, neck, eyesockets, lungs and brain [3]. The information about the magnitude, frequency and duration of vibration and their orientation with respect to the body of subject is very important in analyzing the effects of vibrations/body accelerations on the human body [4, 5]. Hence, it is important to analyze the effects of periodic body accelerations on different parts of the body.

Arteries are narrowed by the development of atherosclerotic plaques that protrude into the lumen, resulting in stenosed arteries [6]. One of the most serious consequences of the stenosis in the arteries is the increased resistance and the associated reduction of the blood flow to the particular vascular bed supplied by the artery [7]. Hence, the presence of a stenosis can lead to the serious circulatory disorder. Long *et al.* [8] and Chakravarthy *et al.* [9] mentioned that the hydrodynamic factors play an important role in the

formation of stenosis [8, 9] and hence, the study of the blood flow through stenosed blood vessels becomes very important.

Many studies were performed to analyze the steady flow of blood, treating it as a Newtonian fluid [10]. It is well known that the blood flow through arteries is highly pulsatile and thus, more attempts have been made to study the pulsatile flow of blood, treating it as a Newtonian fluid [11]. The Newtonian behavior of blood is acceptable only in larger arteries at high shear rates, but, blood, being a suspension of cells in plasma, exhibits remarkable non-Newtonian behavior when it flows through narrow arteries at low shear rates, particularly, in diseased state; the actual flow is distinctly pulsatile [8]. Nagarani and Sarojamma [5] mathematically analyzed the pulsatile flow of Casson fluid for blood flow through stenosed narrow arteries with body acceleration, using perturbation method.

Siddiqui *et al.* [12] reported that Herschel-Bulkley (H-B) fluid model and Casson fluid model are the non-Newtonian fluid models which are used in the studies of blood flow through narrow arteries. Tu and Deville [7] mentioned that blood obeys Casson's equation only for moderate shear rate, whereas the H-B equation can be used still at low shear rates and represents fairly closely what is occurring in blood [9]. Chaturani and Ponnalagar Samy [13] have mentioned that for tube diameter 0.095 mm blood behaves like H-B fluid rather

than power law and Bingham fluids. Hence, it is appropriate to model blood as a H-B fluid model rather than Casson fluid model when it flows in smaller diameter arteries. Hence, in this study, we have mathematical analysis for pulsatile flow of blood through stenosed narrow arteries with body acceleration, treating blood as H-B fluid model.

2. MATHEMATICAL FORMULATION

Consider an axially symmetric, laminar, pulsatile and fully developed flow of blood (assumed to be incompressible) in the \bar{z} direction through a circular narrow artery with stenosis as shown in Figure 1. The segment of the artery under study is considered to be long enough so that the entrance, end and special wall effects can be neglected. Assume that the flow blood is subject to the periodical body acceleration and slip velocity at the wall and the flowing blood is treated as H-B fluid. The cylindrical polar coordinate system $(\bar{r}, \bar{\psi}, \bar{z})$ has been used to analyze the flow.

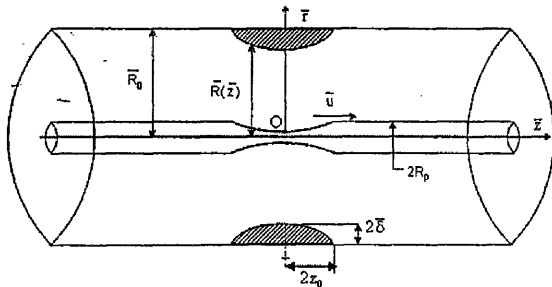


Fig. 1: Geometry of the stenosed artery

It has been reported that the radial velocity is negligibly small and can be neglected for a low Reynolds number flow in a narrow artery with stenosis [6]. The momentum equations governing the flow reduced to,

$$\bar{\rho} \frac{\partial \bar{u}}{\partial \bar{t}} = -\frac{\partial \bar{p}}{\partial \bar{z}} - \frac{1}{\bar{r}} \frac{\partial}{\partial \bar{r}} (\bar{r} \bar{\tau}) + \bar{F}(\bar{t}) \quad \dots (1)$$

$$0 = \frac{\partial \bar{p}}{\partial \bar{r}} \quad \dots (2)$$

where \bar{u} is the axial component of the velocity, \bar{p} is the pressure, $\bar{\rho}$ is the density, \bar{t} is the time, $\bar{\tau} = |\bar{\tau}_{rz}| = -\bar{\tau}_{rz}$ is the shear stress, $\bar{F}(\bar{t})$ is the body acceleration. The constitutive equation of the H-B fluid (which represents the blood) is given by,

$$\bar{\tau} = \bar{\mu}_H \left(\frac{-\partial \bar{u}}{\partial \bar{r}} \right)^{1/n} + \bar{\tau}_H \quad \text{if } \bar{\tau} \geq \bar{\tau}_H \quad \dots (3)$$

$$\frac{\partial \bar{u}}{\partial \bar{r}} = 0 \quad \text{if } \bar{\tau} \leq \bar{\tau}_H \quad \dots (4)$$

where, $\bar{\tau}_H$ is the yield stress and $\bar{\mu}_H$ is the coefficient of viscosity for Herschel-Bulkley fluid with dimension $(ML^{-1}T^{-2})^n T$. The geometry of the stenosis is given by

$$\bar{R}(\bar{z}) = \begin{cases} \bar{R}_0 - \bar{\delta} \left[1 + \cos \left(\frac{\pi \bar{z}}{2\bar{z}_0} \right) \right] & \text{if } |\bar{z}| \leq 2\bar{z}_0 \\ \bar{R}_0 & \text{otherwise} \end{cases} \quad \dots (5)$$

where $\bar{\delta}$ denotes the half of the maximum projection of the stenosis from the wall of the artery to the lumen of the artery such that $\bar{\delta}/\bar{R}_0 \ll 1$, $\bar{R}(\bar{z})$ is the radius of the artery in the stenosed region, \bar{R}_0 is the radius of the normal artery. The boundary conditions are,

$$(i) \bar{\tau} \text{ is finite at } \bar{r} = 0 \quad \dots (6)$$

$$(ii) \bar{u} = 0 \text{ at } \bar{r} = \bar{R}(\bar{z}) \quad \dots (7)$$

Since, the pressure gradient is a function of \bar{z} and \bar{t} , we take

$$-\frac{\partial \bar{p}}{\partial \bar{z}}(\bar{z}, \bar{t}) = A_0 + A_1 \cos(\bar{\omega}_p \bar{t}) \quad \dots (8)$$

where A_0 is the steady component of the pressure gradient, A_1 is the amplitude of the fluctuating component of the pressure gradient and $\bar{\omega}_p = 2\pi \bar{f}_p$, \bar{f}_p is the pulse frequency in Hz. Both A_0 and A_1 are functions of \bar{z} [6]. The periodic body acceleration in the axial direction is given by,

$$\bar{F}(\bar{t}) = a_0 \cos(\bar{\omega}_b \bar{t} + \phi) \quad \dots (9)$$

Where a_0 is the amplitude, $\bar{\omega}_b = 2\pi \bar{f}_b$, \bar{f}_b is the frequency in Hz and is assumed to be small so that the wave effect can be neglected [4], ϕ is the lead angle of $\bar{F}(\bar{t})$ with respect to the heart action. Let us introduce the following non dimensional variables,

$$\begin{aligned} z &= \frac{\bar{z}}{\bar{R}_0}, \quad R(z) = \frac{\bar{R}(\bar{z})}{\bar{R}_0}, \quad r = \frac{\bar{r}}{\bar{R}_0}, \quad t = \bar{t} \bar{\omega}, \\ \omega &= \frac{\bar{\omega}_b}{\bar{\omega}_p}, \quad \delta = \frac{\bar{\delta}}{\bar{R}_0}, \quad u = \frac{\bar{u}}{A_0 \bar{R}_0^2}, \quad \tau = \frac{\bar{\tau}}{A_0 \bar{R}_0}, \\ \theta &= \frac{2\bar{\tau}_H}{A_0 \bar{R}_0}, \quad \alpha^2 = \frac{\bar{R}_0^2 \bar{\omega}_p}{\bar{\mu}_0}, \quad e = \frac{A_1}{A_0}, \quad B = \frac{a_0}{A_0} \quad \dots (10) \end{aligned}$$

Using the non-dimensional variables in Eq. (10), Eqs. (1), (3) and (4) reduced respectively to

$$\alpha^2 \frac{\partial u}{\partial t} = 4(1 + e \cos t) + 4B \cos(\omega t + \phi) - \frac{2}{r} \frac{\partial}{\partial r}(r\tau) \quad \dots (11)$$

$$\tau = \left(-\frac{1}{2} \frac{\partial u}{\partial r}\right)^{1/n} + \theta \quad \text{if } \tau \geq \theta \quad \dots (12)$$

$$\frac{\partial u}{\partial r} = 0 \quad \text{if } \tau \leq \theta \quad \dots (13)$$

The boundary conditions (in the non-dimensional form) are

$$(i) \tau \text{ is finite at } r = 0 \quad \dots (14)$$

$$(ii) u = 0 \text{ at } r = R(z) \quad \dots (15)$$

The geometry of the stenosis in dimensionless form is given by

$$R(z) = \begin{cases} 1 - \delta \left[1 + \cos\left(\frac{\pi z}{2z_0}\right) \right] & \text{if } |z| \leq 2z_0 \\ 1 & \text{otherwise} \end{cases} \quad \dots (16)$$

The non-dimensional volume flow rate $Q(t)$ is given by

$$Q(z,t) = 4 \int_0^{R(z)} u(z,r,t) r dr \quad \dots (17)$$

Where $Q(t) = \bar{Q}(\bar{t}) / [\pi \bar{R}_0^4 A_0 / 8\bar{\mu}]$, $\bar{Q}(\bar{z}, \bar{t})$ is the volumetric flow rate and $\bar{\mu}$ is the viscosity of the Newtonian fluid.

3. METHOD OF SOLUTION

Perturbation method with pulsatile Reynolds number α as the small parameter of the series expansion is used to solve this system of nonlinear partial differential equations. Since, the present study deals with pulsatile flow of blood and when we non-dimensionalize the momentum equation (1), the square of the pulsatile Reynolds number (α^2) occurs naturally, it is more appropriate to expand the Eqs. (11) and (12) in the perturbation series about α^2 . Let us expand the velocity u in the perturbation series about the square of the pulsatile Reynolds number α^2 as below (where $\alpha^2 < 1$).

$$u(r, z, t) = u_0(r, z, t) + \alpha^2 u_1(r, z, t) + \dots \quad \dots (18)$$

Similarly, one can expand the shear stress $\tau(r, z, t)$, the plug core radius $R_p(z, t)$, the plug core velocity

$u_p(z, t)$, and the plug core shear stress $\tau_p(z, t)$ in terms of α^2 . Substituting the perturbation series expansions of u and τ in Eq. (11) and then equating the constant term and α^2 term we get

$$\frac{\partial}{\partial r}(r\tau_0) = 2r[(1 + e \cos t) + B \cos(\omega t + \phi)] \quad \dots (19)$$

$$\frac{\partial u_0}{\partial t} = -\frac{2}{r} \frac{\partial}{\partial r}(r\tau_1) \quad \dots (20)$$

Using the binomial series approximation in Eq. (12) and applying the perturbation series expansions of u and τ in the resulting equation and then equating the constant term and α^2 term, one can obtain

$$-\frac{\partial u_0}{\partial r} = 2\tau_0^{n-1}[\tau_0 - n\theta] \quad \dots (21)$$

$$-\frac{\partial u_1}{\partial r} = 2n\tau_0^{n-2}\tau_1[\tau_0 - (n-1)\theta] \quad \dots (22)$$

Using the perturbation series expansions of u and τ in the boundary conditions (14) and (15), we obtain

$$(i) \tau_0 \text{ and } \tau_1 \text{ are finite at } r = 0 \quad \dots (23)$$

$$(ii) u_0 = 0 \text{ and } u_1 = 0 \text{ at } r = 0 \quad \dots (24)$$

Integrating Eq. (19) between 0 and R_{0p} , and then using the condition that τ_{0p} is finite at $r = 0$, we obtain

$$\tau_{0p} = g(t)R_{0p} \quad \dots (25)$$

Where $g(t) = (1 + e \cos t) + B \cos(\omega t + \phi)$. Integrating Eq. (19) between R_{0p} and r and making use of Eq. (25), one can get,

$$\tau_0 = g(t)r \quad \dots (26)$$

Substituting Eq. (26) into Eq.(21) and integrating between r and $R(= R(z))$ with the help of first of the boundary condition (24), we obtain,

$$u_0 = 2[g(t)R]^n R \left[\frac{1}{(n+1)} \left\{ 1 - \left(\frac{r}{R}\right)^{n+1} \right\} - \left(\frac{q^2}{R}\right) \left\{ 1 - \left(\frac{r}{R}\right)^n \right\} \right] \quad \dots (27)$$

where $q^2 = (\theta/g(t))$. The plug core velocity u_{0p} can be obtained from Eq. (27) as,

$$u_{0p} = 2[g(t)R]^n R \left[\frac{1}{(n+1)} \left\{ 1 - \left(\frac{R_{0p}}{R}\right)^{n+1} \right\} - \left(\frac{q^2}{R}\right) \left\{ 1 - \left(\frac{R_{0p}}{R}\right)^n \right\} \right] \quad \dots (28)$$

Neglecting the terms with α^2 and higher powers of α in the perturbation series expansion of R_p and using Eq. (25), the expression for R_{0p} can be obtained as,

$$r|_{\tau_{0p}=\theta} = R_{0p} = \frac{\theta}{g(t)} = q^2 \quad \dots (29)$$

Using Eq. (29) in Eq. (28), one can get,

$$u_{0p} = 2[g(t)R]^n R \left[\frac{1}{(n+1)} \left\{ 1 - \left(\frac{q^2}{R} \right)^{n+1} \right\} - \left(\frac{q^2}{R} \right) \left\{ 1 - \left(\frac{q^2}{R} \right)^n \right\} \right] \quad \dots (30)$$

Similarly solving Eqs. (20) and (22) with the help of the boundary conditions (23) and (24) and Eqs. (25)–(30), the expressions for τ_{1p} , τ_1 , u_1 and u_{1p} can be obtained as,

$$\tau_{1p} = -[g(t)R]^n DR^2 \left[\frac{n}{2(n+1)} \left(\frac{q^2}{R} \right) - \frac{(n-1)}{2} \left(\frac{q^2}{R} \right)^2 - \frac{n}{2(n+1)} \left(\frac{q^2}{R} \right)^{n+2} \right] \quad \dots (31)$$

$$\tau_1 = -[g(z)R]^n DR^2 \left[\frac{n}{(n+1)(n+3)} \left\{ \left(\frac{n+3}{2} \right) \left(\frac{r}{R} \right) - \left(\frac{r}{R} \right)^{n+2} \right\} - \frac{(n-1)}{(n+2)} \left(\frac{q^2}{R} \right) \left\{ \left(\frac{n+2}{2} \right) \left(\frac{r}{R} \right) - \left(\frac{r}{R} \right)^{n+1} \right\} - \frac{3(n^2+2n-2)}{2(n+2)(n+3)} \left(\frac{q^2}{R} \right)^{n+3} \left(\frac{r}{R} \right) \right] \quad \dots (32)$$

$$u_1 = -2n[g(t)R]^{2n-1} DR^3 \left[\frac{n}{2(n+1)^2(n+3)} \left\{ (n+2) - (n+3) \left[\frac{r}{R} \right]^{n+1} + \left[\frac{r}{R} \right]^{2n+2} \right\} + \frac{(n-1)}{2(n+1)(n+2)(n+3)(2n+1)} \left[\frac{q^2}{R} \right] \left\{ (n+2)(n+3)(2n+1) \left[\left(\frac{r}{R} \right)^n + \left(\frac{r}{R} \right)^{n+1} \right] - 2 \left[(2n^3+9n^2+11n+3) + (2n^2+6n+3) \left[\frac{r}{R} \right]^{2n+1} \right] \right\} + \frac{(n-1)^2}{2n(n+2)} \left(\frac{q^2}{R} \right)^2 \left\{ (n+1) - (n+2) \left[\frac{r}{R} \right]^n + \left[\frac{r}{R} \right]^{2n} \right\} \right]$$

$$+ \frac{3(n^2+2n-2)}{2(n-1)(n+2)(n+3)} \left(\frac{q^2}{R} \right)^{n+3} \left\{ \left(\frac{r}{R} \right)^{n-1} - 1 \right\} + \frac{3(n^2+2n-2)(n-1)}{2(n-2)(n+2)(n+3)} \left(\frac{q^2}{R} \right)^{n+4} \left\{ 1 - \left[\frac{r}{R} \right]^{n-2} \right\} \quad \dots (33)$$

$$u_{1p} = -2n[g(t)R]^{2n-1} DR^3 \left[\frac{n}{2(n+1)^2(n+3)} \left\{ (n+2) - (n+3) \left[\frac{q^2}{R} \right]^{n+1} + \left[\frac{q^2}{R} \right]^{2n+2} \right\} + \frac{(n-1)}{2(n+1)(n+2)(n+3)(2n+1)} \left[\frac{q^2}{R} \right] \left\{ (n+2)(n+3)(2n+1) \left[\left(\frac{q^2}{R} \right)^n + \left(\frac{q^2}{R} \right)^{n+1} \right] - 2 \left[(2n^3+9n^2+11n+3) + (2n^2+6n+3) \left[\frac{q^2}{R} \right]^{2n+1} \right] \right\} + \frac{(n-1)^2}{2n(n+2)} \left(\frac{q^2}{R} \right)^2 \left\{ (n+1) - (n+2) \left[\frac{q^2}{R} \right]^n + \left[\frac{q^2}{R} \right]^{2n} \right\} + \frac{3(n^2+2n-2)}{2(n-1)(n+2)(n+3)} \left(\frac{q^2}{R} \right)^{n+3} \left\{ \left(\frac{q^2}{R} \right)^{n-1} - 1 \right\} + \frac{3(n^2+2n-2)(n-1)}{2(n-2)(n+2)(n+3)} \left(\frac{q^2}{R} \right)^{n+4} \left\{ 1 - \left[\frac{q^2}{R} \right]^{n-2} \right\} \right] \quad \dots (34)$$

where $D = (1/g)(dg/dt)$. The wall shear stress τ_w is a physiologically important quantity which plays an important role in determining aggregate sites of platelets [11]. The expression for wall shear stress τ_w is given by,

$$\tau_w = \left(\tau_0 + \alpha^2 \tau_1 \right)_{r=R} = [g(t)R] \left[1 - \frac{(g(t)R)^{n-1} \alpha^2 R^2 B}{2(n+2)(n+3)} \left\{ n(n+2) - (n-1)n(n+3) \left(\frac{q^2}{R} \right) - 3(n^2+2n-2) \left(\frac{q^2}{R} \right)^{n+3} \right\} \right] \quad \dots (35)$$

From Eq. (17) and the expressions for velocity, one can derive the expression for the volumetric flow rate $Q(z, t)$ as,

$$\begin{aligned}
 Q(z, t) &= 4 \left[\left(\int_0^{R_{0p}} r u_{0p} dr + \int_{R_{0p}}^R r u_0 dr \right) \right. \\
 &\quad \left. + \alpha^2 \left(\int_0^{R_{0p}} r u_{1p} dr + \int_{R_{0p}}^R r u_1 dr \right) \right] \\
 &= \frac{[g(t)R]^n R^3}{(n+2)(n+3)} \\
 &\quad \left[\left\{ (n+2) - n(n+3) \left(\frac{q^2}{R} \right) + (n^2 + 2n - 2) \left(\frac{q^2}{R} \right)^{n+3} \right\} \right. \\
 &\quad \left. - \alpha^2 [g(t)R]^{n-1} \left(\frac{nDR^2}{4} \right) \right. \\
 &\quad \left\{ n - \frac{2n(n-1)(4n^2 + 12n + 5)}{(2n+1)(2n+3)} \left(\frac{q^2}{R} \right) \right. \\
 &\quad \left. + \frac{n(n-1)^2(n+3)}{(n+1)} \left(\frac{q^2}{R} \right)^2 + \frac{(n^3 - 2n^2 - 11n + 6)}{(n+1)} \left(\frac{q^2}{R} \right)^{n+3} \right. \\
 &\quad \left. - \frac{(n-1)(n^3 - 2n^2 - 11n + 6)}{n} \left(\frac{q^2}{R} \right)^{n+4} \right. \\
 &\quad \left. \left. - \frac{(4n^5 + 14n^4 - 8n^3 - 45n^2 - 3n + 18)}{n(n+1)(2n+3)} \left(\frac{q^2}{R} \right)^{2n+4} \right\} \right] \\
 &\quad \dots (36)
 \end{aligned}$$

The correction to the plug core radius R_{1p} can be obtained by neglecting the terms with α^4 and higher powers of α in the perturbation series expansion of R_p in the following manner. The shear stress $\tau = \tau_0 + \alpha^2 \tau_1$ at $r = R_p$ is given by,

$$\left[\tau_0 + \alpha^2 \tau_1 \right]_{r=R_p} = \theta \quad \dots (37)$$

From the Taylor's series of τ_0 and τ_1 about R_{0p} and $\tau_0|_{r=R_{0p}} = \theta$, one can obtain,

$$R_{1p} = \left(-\tau_1|_{r=R_{0p}} \right) / g(t) \quad \dots (38)$$

Substitution of Eqs. (26) and (38) in the perturbation series expansion of R_p yields,

$$\begin{aligned}
 R_p &= q^2 + \alpha^2 [g(t)R]^{n-1} \\
 &\quad \left(\frac{nDR^3}{2(n+1)} \right) \left[\left(\frac{q^2}{R} \right) - \left(\frac{n^2-1}{n} \right) \left(\frac{q^2}{R} \right)^2 - \left(\frac{q^2}{R} \right)^{n+2} \right] \\
 &\quad \dots (39)
 \end{aligned}$$

The longitudinal impedance of the artery is given by,

$$\Lambda = g(t) / Q(z, t) \quad \dots (40)$$

4. NUMERICAL SIMULATION OF THE RESULTS

The aim of this study is to bring out the effects of the body acceleration, pulsatility of the flow, non-Newtonian nature of the blood and pressure gradient on the plug core radius, plug flow velocity, velocity, wall shear stress, flow rate and longitudinal impedance to flow. The flowing blood is modeled as H-B fluid model. The values of the power law index 'n' for blood flow problems are generally taken to lie between 0.9 and 1.1 and in this analysis, we have used the value of n as 0.95 for $n < 1$ and 1.05 for $n > 1$ [14]. The values of the non-dimensional yield stress θ for the blood of the normal subject are between 0.01 and 0.04 and in the diseased state, it is quite high and in such a case, the value of the yield stress is taken to lie between 0.05 and 0.2 [13]. The origin of the coordinate system is fixed at the middle of the stenosis where the stenosis projection is maximum. The stenosis is assumed to lie between $z = -2Z_0$ and $z = 2Z_0$. The pressure gradient parameter 'e' is taken in the range 0.5–0.7 [5]. The value of pulsatile Reynolds number is generally taken as 0.2 and only to pronounce its effect, we have taken the range 0.2–0.7 [12]. To discuss the effects of the body acceleration parameter B on the various flow quantities, its value is taken in the range 0–2 [6].

4.1 Plug Core Radius

The variation of the plug core radius in a time cycle for different values of B, e and θ with $\alpha = \phi = 0.2$, $n = 0.95$ and $\delta = 0.15$ is depicted in Figure 2. It is seen that the plug core radius increases very slowly as the time parameter t increases from 0° to 90° and then it increases rapidly as the time t increases from 90° to 120° and then it decreases as t increases from 120° to 180° and then it increases nonlinearly as t increases from 180° to 210° and then it decreases rapidly as the time t increases from 210° to 240° and then it decreases

very slowly as time t increases further from 240° to 360°

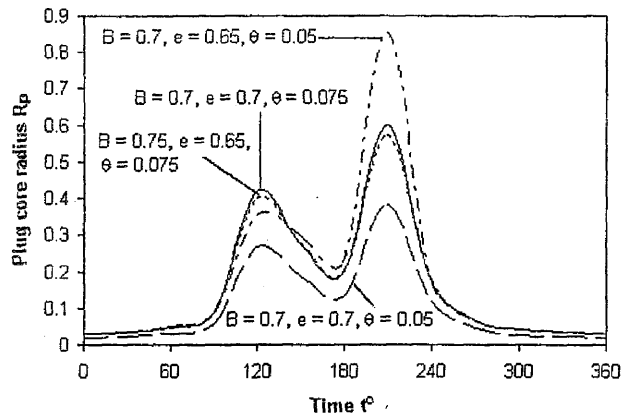


Fig. 2: Variation of plug core radius in a time cycle for different values of B , e and θ with $\alpha = \phi = 0.2$, $n = 0.95$ and $\delta = 0.15$

It is observed that for a given set of values of B and e and increasing values of the yield stress θ , the plug core radius increases marginally when time t lies between 0° and 90° and also between 240° and 360° and increases significantly when time t lies between 90° and 240° . The plug core radius decreases with the increase of either body acceleration parameter B or the pressure gradient e when all the other parameters were held constant.

4.2 Plug Flow Velocity

The variation of the plug flow velocity in a time cycle for different values of B , θ and α with $n = 0.95$, $e = 0.5$, $\phi = 0.2$, $\delta = 0.1$ and $\omega = 1$ is illustrated in Figure 3. It is clear that in the presence of the body acceleration, the plug flow velocity decreases rapidly with the increase of the time t from 0° to 120° and then it increases slowly when time t increases from 120° to 180° and then it decreases as time t increases from 180° to 210° and then it increases rapidly when time t increases from 210° to 360° . It is found that the plug flow velocity increases with the increase of the body acceleration when time t lies between 0° and 90° , 150° and 200° , and also between 270° and 360° and it decreases in the rest of the time cycle. It is seen that the plug flow velocity decreases marginally with the increase of the yield stress when all the other parameters were held constant.

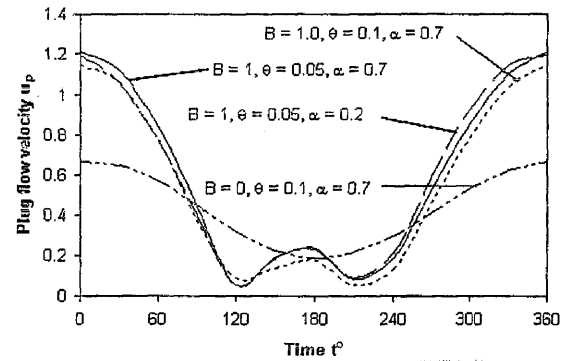


Fig. 3: Variation of plug flow velocity in a time cycle for different values of B , θ and α

with $n = 0.95$, $e = 0.5$, $\phi = 0.2$, $\delta = 0.1$ and $\omega = 1$

4.3 Velocity Distribution

Velocity distribution for different fluid models with $\phi = \alpha = 0.2$, $\delta = 0.1$, $B = t = \omega = 1.0$ and $e = 0.5$ is shown in Figure 4.

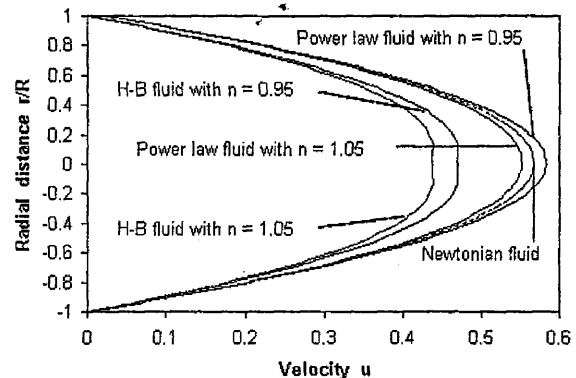


Fig. 4: Velocity distribution for different fluid models with $\theta = 0.1$, $\delta = 0.2$, $\phi = \alpha = 0.2$,

$\omega = 1$, $t = 1$, $e = 0.5$ and $B = 1.0$

It is observed that the velocity decreases marginally with the increase of the power law index and yield stress. It is of importance to note that the plot of the Newtonian fluid model is in good agreement with Figure 4 of Nagarani and Sarojamma [5]. It is noticed that the velocity is maximum for the power law fluid with $n = 0.95$ and minimum for the H-B fluid model with $n = 1.05$.

4.4 Wall Shear Stress

The variation of wall shear stress in a time cycle for different values of B , e and α with $\omega = 1$, $n = 0.95$,

$\phi = 0.2$, $\theta = 0.05$ and $\delta = 0.1$ is sketched in Figure 5. It is seen that in the presence of the body acceleration, the wall shear stress decreases rapidly with the increase of the time t from 0° to 120° and then it increases slowly when time t increases from 120° to 180° and then it decreases as time t increases from 180° to 210° and then it increases rapidly when time t increases from 210° to 360° . It is found that for fixed values of e and α and the increasing values of the body acceleration parameter B , the wall shear stress increases when time t lies between 0° and 90° , 150° and 200° , and also between 270° and 360° and it decreases in the rest of the time cycle. For a given set of values of B and e and increasing values of the pulsatile Reynolds number α , the wall shear increases slightly when the time t lies between 0° and 180° and it decreases when the time t lies between 180° and 360° .

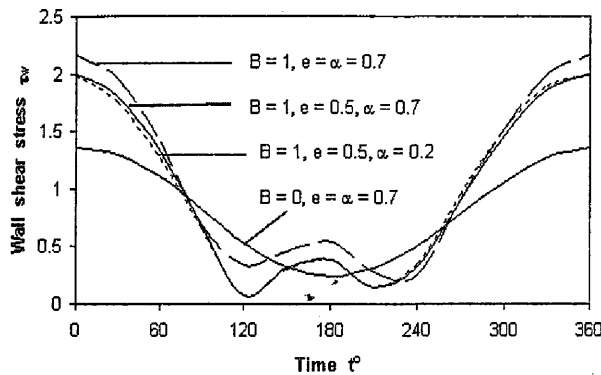


Fig. 5: Variation of wall shear stress in a time cycle for different values of B , e and α with $\omega = 1$, $n = 0.95$, $\phi = 0.2$, $\theta = 0.05$ and $\delta = 0.1$

4.5 Longitudinal Impedance

The variation of the longitudinal impedance with the stenosis depth for different values of α , B and θ with $\phi = 0.2$, $n = 0.95$, $\omega = 1$ and $t = 60^\circ$ is shown in Figure 6. It is found that the longitudinal impedance increases slowly with the increase stenosis δ depth from 0 to 0.15 and then it increases nonlinearly (rapidly) when the stenosis depth δ increases further from 0.15 to 0.25. It is noted that for the fixed value of the yield stress θ , the longitudinal impedance decreases with the increase of either the body acceleration parameter B or the pulsatile Reynolds number α , but the decrease in the longitudinal impedance is marginal when the pulsatile Reynolds number α increases and is considerable when the body acceleration parameter B increases. For a given set of values of B and α , the longitudinal

impedance increases considerably when the yield stress θ increases.

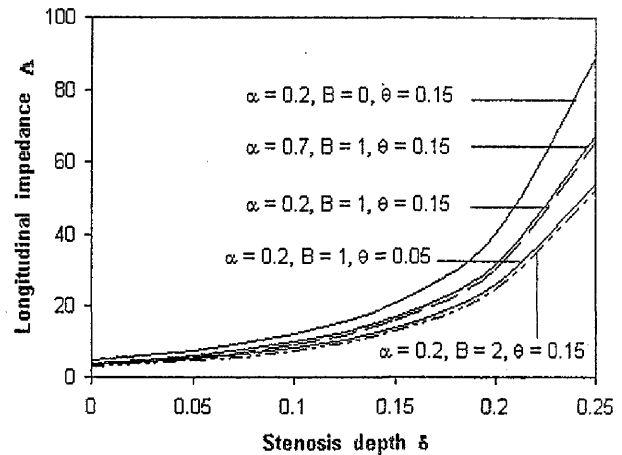


Fig. 6: Variation of longitudinal impedance with stenosis depth for different values of α , B and θ with $\alpha = \phi = 0.2$, $n = 0.95$, $\omega = 1.0$ and $t = 60^\circ$

5. CONCLUSIONS

The present theoretical analysis discussed interesting rheological properties of blood when it flows through narrow stenosed artery with body acceleration, treating it as a H-B fluid. It is noted that the plug core radius decreases with the increase of the body acceleration parameter B and the pressure gradient e and, it increases with the increase of the yield stress, power law index and depth of the stenosis. It is observed that the velocity decreases marginally with the increase of the power law index, yield stress, depth of the stenosis and lead angle of the body acceleration and, it increases with the increase of the body acceleration, the pulsatile Reynolds number, the pressure gradient. It is observed that the longitudinal impedance increases with the increase of the stenosis depth δ and yield stress θ and, it decreases with the increase of the body acceleration and the pulsatile Reynolds number.

REFERENCES

- [1] Sud, V.K. and Sekhon, G.S. Arterial flow under periodic body acceleration, Bulletin of Mathematical Biology 47 (1985) 35–52.
- [2] Usha, R. and Prema, K. Pulsatile flow of particle-fluid suspension model of blood under periodic body acceleration, ZAMP 50 (1999) 175–192.
- [3] Chaturani, P. and Palanisami, V. Casson fluid model of pulsatile flow of blood flow under periodic body acceleration, Biorheology 27 (1990) 619–630.

- [4] Chaturani, P. and Palanisami, V. Pulsatile flow of power law fluid model for blood flow under periodic body acceleration, *Biorheology* 27 (1990) 747–758.
- [5] Nagarani, P. and Sarojamma, G. Effect of body acceleration on pulsatile flow of Casson fluid through a mild stenosed artery, *Korea-Australia Rheology Journal* 20 (2008) 189–196.
- [6] Chaturani, P. and Samy, R. Ponnalagar, Pulsatile flow of Casson's fluid through stenosed arteries with applications to blood flow, *Biorheology* 23 (1986) 499–511.
- [7] Tu, C. and Deville, M. Pulsatile flow of non-Newtonian fluids through arterial stenosis, *Journal of Biomechanics* 29 (1996) 899–908.
- [8] Long, Q., Ku, X.Y., Ramnarine, K.V. and Hoskins, P. Numerical investigations of physiologically realistic pulsatile flow through arterial stenosis, *Journal of Biomechanics* 34 (2001) 1229–1242.
- [9] Chakravarthy, S., Datta, A. and Mandal, P.K. Analysis of nonlinear blood flow in a stenosed flexible artery, *International Journal of Engineering Science* 33 (1995) 1821–1837.
- [10] Texon, M. The hemodynamic concept of atherosclerosis, *Bulletin of the New York Academy of Medicine* 36 (1960) 263–273.
- [11] Sarkar, A. and Jayaraman, G. Correction to flow rate-pressure drop relation in coronary angioplasty: steady streaming effect, *Journal of Biomechanics* 31 (1998) 781 - 791.
- [12] Siddiqui, S.U., Verma, N.K., Mishra, Shailesh and Gupta, R.S. Mathematical modeling of pulsatile flow of Casson's fluid in arterial stenosis, *Applied Mathematics and Computation* 210 (2009) 1-10.
- [13] Chaturani, P. and Samy, R. Ponnalagar, A study of non-Newtonian aspects of blood flow through stenosed arteries and its applications in arterial diseases, *Biorheology* 22 (1985) 521–531.
- [14] Sankar, D.S. and Lee, Usik, Two -fluid nonlinear mathematical model for pulsatile blood flow through catheterized arteries, *Journal of Mechanical Science and Technology* 23 (2009) 1650–1669.